AD-A114 043

CONTRACT REPORT ARBRL-CR-00478

ANALYSIS OF A RAIL GUN PLASMA ACCELERATOR

Prepared by

Science Applications, Inc.
6600 Powers Ferry Rd., Suite 220
Atlanta, GA 30339

April 1982

US ARMY ARMAMENT RESEARCH AND DEVELOPMENT COMMAND
BALLISTIC RESEARCH LABORATORY
ABERDEEN PROVING GROUND, MARYLAND

Destroy this report when it is no longer needed.
Do not return it to the originator.

Secondary distribution of this report by originating or sponsoring activity is prohibited.

Additional copies of this report may be obtained from the National Technical Information Service, U.S. Department of Commerce, Springfield, Virginia 22161.

The findings in this report are not to be construed as an official Department of the Army position, unless so designated by other authorized documents.

The use of trade names or manufacturers' names in this report does not constitute indorsement of any commercial product.

UNCLASSIFIED

SECURITY CLASSIFICATION OF THIS PAGE *(When Data Entered)*

REPORT DOCUMENTATION PAGE		READ INSTRUCTIONS BEFORE COMPLETING FORM
1. REPORT NUMBER Contract Report ARBRL-CR-00478	2. GOVT ACCESSION NO.	3. RECIPIENT'S CATALOG NUMBER
4. TITLE *(and Subtitle)* Analysis of a Rail Gun Plasma Accelerator		5. TYPE OF REPORT & PERIOD COVERED Final
		6. PERFORMING ORG. REPORT NUMBER
7. AUTHOR*(s)* Jad H. Batteh		8. CONTRACT OR GRANT NUMBER*(s)* DAAK11-80-C-0102
9. PERFORMING ORGANIZATION NAME AND ADDRESS Science Applications, Inc. 6600 Powers Ferry Rd., Suite 220 Atlanta, GA 30339		10. PROGRAM ELEMENT, PROJECT, TASK AREA & WORK UNIT NUMBERS RDT&E 1L162603AH18
11. CONTROLLING OFFICE NAME AND ADDRESS US Army Armament Research & Development Command US Army Ballistic Research Laboratory (DRDAR-BL) Aberdeen Proving Ground, MD 21005		12. REPORT DATE April 1982 13. NUMBER OF PAGES 53
14. MONITORING AGENCY NAME & ADDRESS*(if different from Controlling Office)*		15. SECURITY CLASS. *(of this report)* Unclassified 15a. DECLASSIFICATION/DOWNGRADING SCHEDULE

16. DISTRIBUTION STATEMENT *(of this Report)*

Approved for public release; distribution unlimited.

17. DISTRIBUTION STATEMENT *(of the abstract entered in Block 20, if different from Report)*

18. SUPPLEMENTARY NOTES

19. KEY WORDS *(Continue on reverse side if necessary and identify by block number)*

Electric gun, rail gun, plasma accelerator, electromagnetic propulsion, plasma dynamics, fluid mechanics

20. ABSTRACT *(Continue on reverse side if necessary and identify by block number)*

A model is developed to study the characteristics of an arc-driven rail gun. In particular, a system of equations is developed which provides a computationally efficient method for estimating the arc-projectile acceleration and the average thermodynamic properties of the arc. Predictions of the model are compared with experimental measurements and with the results of other investigations. The model is used to determine the range of plasma conditions which can be achieved through variations of the arc mass, projectile mass and current. The possibility of using the rail gun as a plasma accelerator is discussed with particular

DD FORM 1 JAN 73 1473 EDITION OF 1 NOV 65 IS OBSOLETE

UNCLASSIFIED

SECURITY CLASSIFICATION OF THIS PAGE *(When Data Entered)*

emphasis on the range limitations imposed by plasma expansion.

TABLE OF CONTENTS

LIST OF FIGURES

LIST OF TABLES

I. INTRODUCTION

In recent years, there has been considerable interest in the electromagnetic acceleration of projectiles, resulting primarily from the successful series of rail gun experiments performed by Marshall and his co-workers at the Australian National University [1-3]. With a homopolar generator to power their device, they were able to accelerate a 3 g projectile to a velocity of 6 km/s in a distance of 3 m [1]. Recognizing the potential benefits of rail gun technology, DARPA and the Army have embarked on a program to advance the state-of-the-art of electromagnetic acceleration. A major component of this program is a project underway at Westinghouse to design and build a rail gun capable of accelerating a 300 g mass to 3 km/s in a distance of 3 m.

Figure 1 shows a schematic representation of a typical rail gun, which consists of two parallel, stationary conductors which are bridged by a mobile armature adjacent to a projectile. When a potential is applied to the rails, a current I passes down one rail through the armature and back up the other rail. This creates a magnetic field in the region bounded by the rails and armature. The interaction of this field with the current through the armature generates a force which accelerates the armature, and thus the projectile, down the rails. For relatively low current experiments, the armature can be a solid conductor. However, as the current is increased to achieve higher accelerations, there is a tendency for the armature to melt as a result of the increased ohmic heating. To circumvent this problem, a plasma arc is generally used as the armature for high current rail guns. In fact, the highest accelerations to date were achieved by Marshall and Rashleigh with an arc driven rail gun [1].

In this report, we focus primarily on the use of the rail gun as a plasma accelerator. A plasma accelerator would have a number of potential applications. For example, it could form the basis for a low thrust, high specific impulse propulsion mechanism. In addition, the combination of high temperatures and velocities attainable

---

1. S. C. Rashleigh and R. A. Marshall, "Electromagnetic Acceleration of Macroparticles to High Velocities," J. Appl. Phys. 49, 2540 (1978).
2. R. A. Marshall, "The Australian National University Rail Gun Project," Atomic Energy, 16, January 1975.
3. J. P. Barber, "The Acceleration of Macroparticles and a Hypervelocity Electromagnetic Accelerator," Ph.D. Thesis (Australian National University, 1972) (Unpublished).

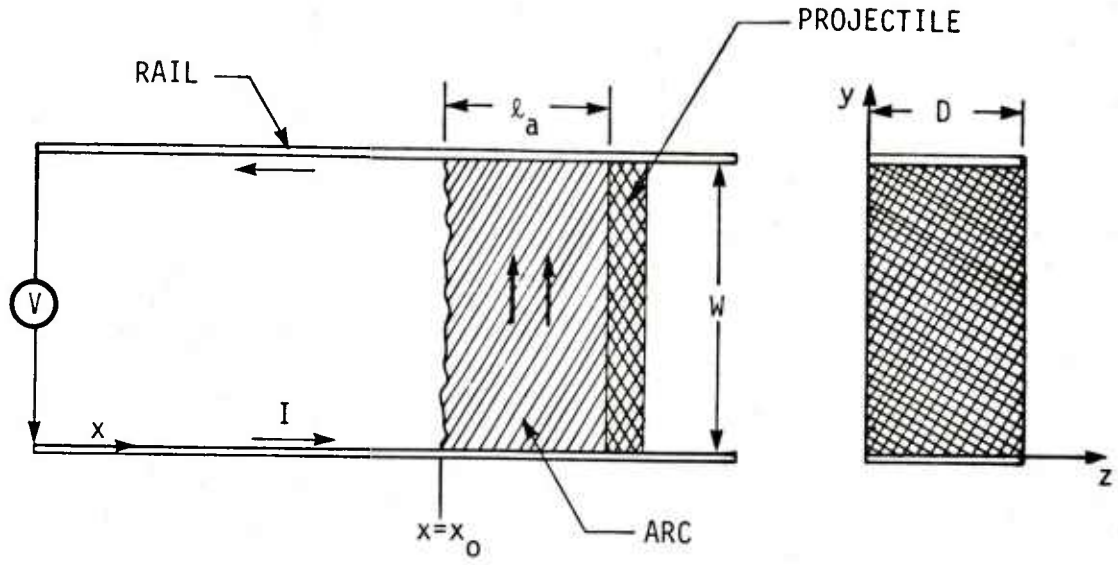

Figure 1. Model for Rail Gun Analysis

with this device would make it ideal for applying coatings to surfaces. As a research tool, the plasma accelerator could be used for studying energy transfer processes in plasmas, for example, through colliding plasma experiments analogous to the colliding beam experiments commonly undertaken. If sufficiently high energies can be attained, the plasma accelerator may even be useful as an injector for a fusion device. Finally, if the hot plasma could be kept confined and propagated for a significant distance through the atmosphere, then the plasma accelerator would also have obvious military significance.

The plasma accelerator which will be analyzed in this report is actually identical to a conventional arc-driven rail gun in that the plasma is used to accelerate a projectile down the rails. The purpose of the projectile is to provide an inertial force which keeps the plasma confined to a reasonably small volume in the gun. The projectile would then be removed from the path of the plasma at the muzzle.

The primary purpose of this analysis will be to determine the range of plasma temperatures, pressures, and accelerations, as well as arc lengths, which can be obtained by varying the arc mass, the projectile mass and the current in the rail gun. In addition, we will derive an expression to estimate the effective range of the plasma in the atmosphere.

The report is organized as follows. In Section II we present the rail gun model used in the analysis. In Section III we use the model to calculate the properties of the plasma for operating conditions typical of the Rashleigh-Marshall (RM) experiment and compare the results with both the experiment and previous studies. In Section IV we explore the range of plasma parameters which can be obtained by varying the operating parameters in the RM experiment. A calculation of the arc properties for the proposed Westinghouse experiment, for a range of values of the arc mass, is presented in Section V. Section VI contains a discussion of the effective range of the plasma in the atmosphere and its impact on potential applications for the plasma accelerator. Finally, in Section VII we present a summary of the results of this effort and recommendations for future studies.

II. RAIL GUN MODEL

For this analysis we will assume that the arc and projectile have reached a "steady state" in the sense that the acceleration of the projectile and all parts of the arc are independent of time and that the fluid mechanical properties of the arc are independent of time in a frame which accelerates with the arc. Necessary conditions for the steady state approximation to be valid are discussed in detail in Reference 4. Here we only note that in order to achieve a steady state the acceleration time t must be long enough for the current to diffuse throughout the arc plasma and for the plasma to achieve its equilibrium temperature and pressure distribution.

The model which will be developed in this section is not intended to provide detailed profiles for the gasdynamic properties of the arc. Rather, our intent has been to develop a computationally efficient, physically transparent model which can be used to estimate the average arc properties for a wide range of operating conditions. Thus, a number of simplifications have been introduced into the calculation. The effect of these simplifications on the predictions of the model will be addressed in this section as well as in Section III where we attempt to model the RM experiment.

A. Arc Pressure and Acceleration

The equations we will use to determine the electromagnetic fields and the plasma pressure are based on the one-dimensional analysis of an arc-driven rail gun presented by Powell and Batteh [4,5]. In that analysis the electromagnetic fields and the gasdynamic properties of the plasma were assumed to depend only on the axial coordinate, x (see Figure 1). In addition, the electromagnetic fields in the arc were calculated assuming the height of the rails was infinite. The one-dimensional approximation for the electromagnetic fields is reasonable throughout most of the arc provided that the rail height D is sufficiently large. We note, however, that the use of infinitely

---

4. J. D. Powell and J. H. Batteh, "Plasma Dynamics of an Arc-Driven, Electromagnetic Projectile Accelerator," J. Appl. Phys. 52, 2717 (1981).
5. J. D. Powell and J. H. Batteh, "Plasma Dynamics of the Arc-Driven Rail Gun," Ballistic Research Laboratory Report No. ARBRL-TR-02267, 1980. (AD A092345)

high rails will lead to an overestimate of the force on the projectile.

In the analysis of Reference 4 it was observed that the arc pressure and density were strongly dependent on position in the arc, due to the purely mechanical effect of accelerating the projectile, whereas the arc temperature, conductivity and degree of ionization were considerably less sensitive to position. Therefore, for this analysis, we assume that the temperature, conductivity and degree of ionization are constant throughout the arc, while the pressure and density are allowed to vary with axial position in the arc.

The pressure in the arc is determined from the momentum equation which, in a reference frame accelerating with the arc, reduces to [4]

$$\frac{dp}{d\xi} = \ell_a [JB - \rho a] \tag{1}$$

where p is the pressure, ℓ_a is the arc length, J is the magnitude of the current density in the arc, B is the magnitude of the magnetic induction, ρ is the density and a is the common acceleration of the arc and projectile. The axial coordinate in the accelerating frame has been normalized according to the definition

$$\xi = \frac{x - x_o}{\ell_a} \tag{2}$$

so that ξ varies from zero at the back of the arc to unity at the projectile.

The current density and magnetic induction are given by

$$J = \frac{\sigma(\xi) j}{\ell_a \bar{\sigma}} \tag{3}$$

and

$$B = \frac{\mu j}{\bar{\sigma}} \int_{\xi}^{1} \sigma(\xi) d\xi \ , \tag{4}$$

respectively, where σ is the plasma conductivity, $\bar{\sigma}$ is the average conductivity in the plasma,

$$\bar{\sigma} = \int_{0}^{1} \sigma(\xi) d\xi \ , \tag{5}$$

μ is the magnetic permeability, and

$$j = \ell_a \int_0^1 J(\xi)d\xi \tag{6}$$

is the current per unit height on the rails. If we take the conductivity to be constant, then $\sigma = \bar{\sigma}$ and Equations (3) and (4) reduce to

$$J = j/\ell_a \tag{7}$$

and

$$B = \mu j(1 - \xi) \ . \tag{8}$$

The plasma density is related to the temperature and pressure through the equation of state

$$p = (1 + \alpha)\rho k_b T/m_o \tag{9}$$

where α is the ratio of electrons to heavy particles (ions plus neutrals), k_b is Boltzmann's constant and m_0 is the atomic mass of the ion or neutral. If we assume that the degree of ionization and the temperature are constant with values $\bar{\alpha}$ and $\bar{T}$, respectively, corresponding to their average values in the arc, then the density is directly proportional to the pressure

$$\rho = \frac{m_o}{(1 + \bar{\alpha})k_b\bar{T}} p \ . \tag{10}$$

Substituting Equations (7), (8), and (10) into Equation (1) yields the equation

$$\frac{dp}{d\xi} + C_1 p = \mu j^2(1 - \xi) \tag{11}$$

where

$$C_1 = \frac{a\ell_a m_o}{k_b(1 + \bar{\alpha})\bar{T}} \ . \tag{12}$$

The solution to Equation (11) subject to the boundary condition

$$p(0) = 0 \tag{13}$$

is

$$p(\xi) = \frac{\mu j^2}{C_1}\left[\left(1+\frac{1}{C_1}\right)\left(1-e^{-C_1\xi}\right)-\xi\right]. \tag{14}$$

Since the final pressure p_f must equal the force per unit area on the projectile, we have the relationships

$$p_f = p(1) = \frac{am_p}{WD} = \mu j^2 f(C_1) \tag{15}$$

where m_p is the mass of the projectile and the function $f(C_1)$ is given by

$$f(C_1) = \frac{1}{C_1}\left[\frac{1}{C_1}\left(1-e^{-C_1}\right)-e^{-C_1}\right]. \tag{16}$$

Equation (15) in its present form cannot be solved directly for the acceleration since C_1 is a function of both a and ℓ_a which are unknown. To uncouple these parameters, we note that the arc mass is given by

$$m_a = \ell_a WD \int_0^1 \rho(\xi)\,d\xi \tag{17}$$

which can be written, with the substitution of Equations (10) and (12), as

$$m_a = \frac{WDC_1}{a}\,\bar{p} \tag{18}$$

where

$$\bar{p} = \int_0^1 p(\xi)\,d\xi$$

is the average pressure in the arc. The average pressure is calculated most easily from the differential equation, Equation (11), with the result

$$\bar{p} = \frac{1}{C_1}\left(\frac{1}{2}\mu j^2 - p_f\right) . \tag{19}$$

Substituting Equations (19) and (15) into Equation (18) and rearranging the terms yields the expression

$$a = \frac{\mu j^2 WD}{2(m_a + m_p)} \tag{20}$$

for the acceleration of the arc and projectile.

Substituting Equation (20) for the acceleration into Equation (15) yields the expression

$$f(C_1) = \frac{m_p}{2(m_p + m_a)} \, . \tag{21}$$

Thus, the parameter C_1, which relates the arc length, the acceleration, and the temperature according to Equation (12), is a function only of the ratio of the arc mass to the projectile mass. Figure 2 shows the dependence of both C_1 and $f(C_1)$ on the arc mass ratio, m_a/m_p. For most rail gun applications $m_a/m_p << 1$ and C_1 and $f(C_1)$ can be approximated by

$$C_1 = \frac{3m_a}{2m_p} \tag{22}$$

$$f(C_1) = \frac{1}{2} - \frac{C_1}{3} \, .$$

Once C_1 is determined from Equation (21) for a given m_a/m_p, the pressure profile can be obtained from Equation (14).

The final and average arc pressures can now be readily evaluated. Equations (15) and (20) yield

$$p_f = \frac{\mu j^2 m_p}{2(m_a + m_p)} \tag{23}$$

for the arc pressure at the projectile. Substituting Equation (23) into Equation (19) yields

$$\bar{p} = \frac{\mu j^2 m_a}{2C_1(m_a + m_p)} \tag{24}$$

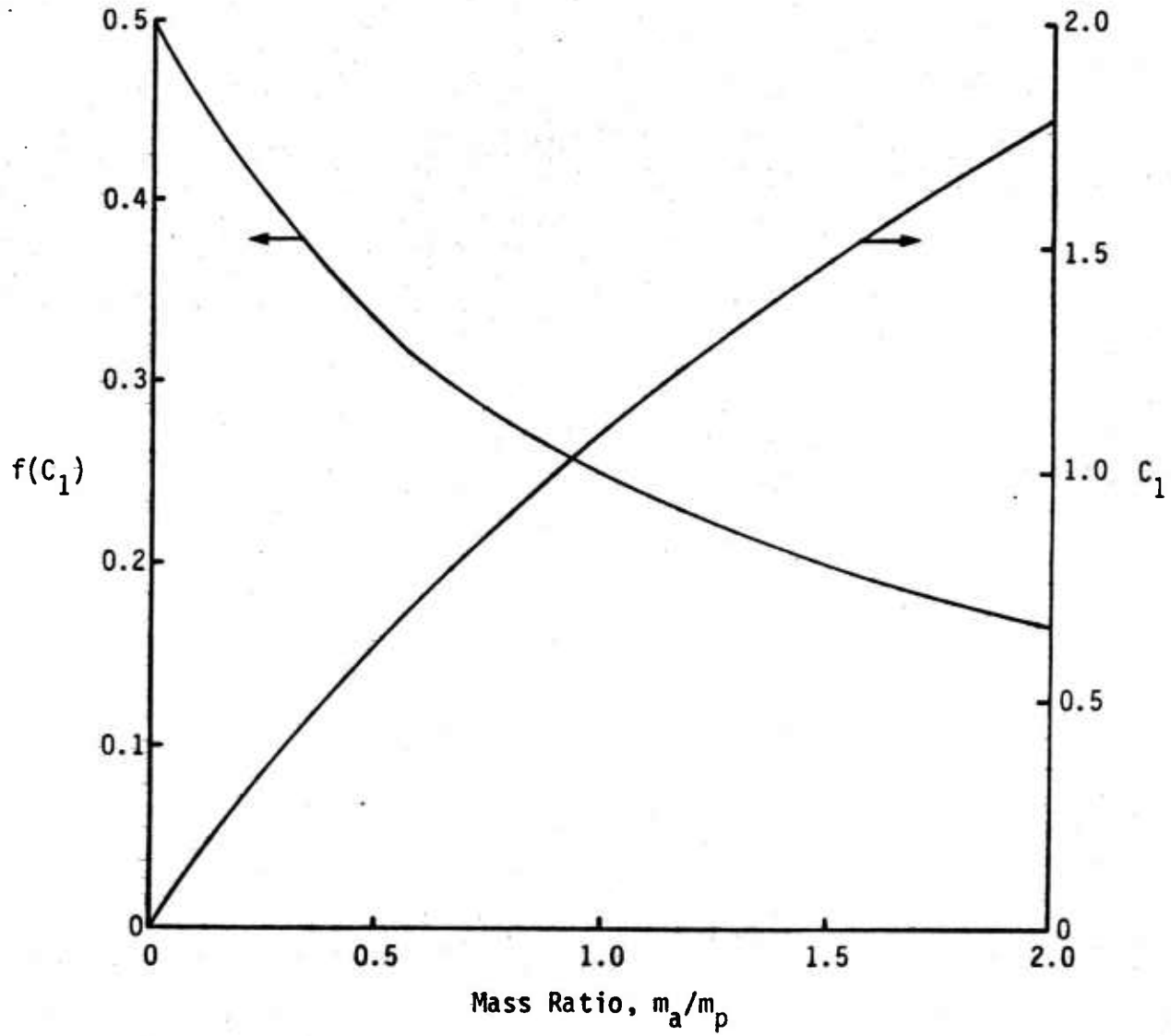

Figure 2. Variation of C_1 and $f(C_1)$ with Arc Mass Ratio

for the average arc pressure. Thus, for this model, the acceleration and the pressure profile in the plasma can be determined without having to solve for the arc temperature.

It is interesting to note that Equation (14) predicts that the maximum pressure in the arc occurs not at the projectile but at

$$\xi_m = \frac{\ln(1 + C_1)}{C_1}$$

where it has the value

$$p_{max} = \frac{\mu j^2}{C_1} \left[1 - \frac{1}{C_1} \ln(1 + C_1)\right] .$$

As the mass ratio $m_a/m_p \to 0$, however, ξ_m approaches unity and, consequently, p_{max} approaches p_f.

B. Arc Temperature and Length

Equation (12) provides a relationship for the ratio of the arc length to the average temperature in terms of the acceleration and the mass ratio, m_a/m_p. To determine either quantity explicitly one additional relationship is needed. This relationship is provided by the energy equation which, for a steady arc in the accelerating frame, reduces to

$$\vec{\nabla} \cdot \vec{q} = \frac{J^2}{\bar{\sigma}} \qquad (25)$$

where $\vec{q}$ is the heat flux. Equation (25) represents the principle that, in the steady state, the ohmic heating must be balanced by the heat loss for every point in the arc.

In writing Equation (25) we have neglected the contribution of any internal flow in the arc to the energy balance. Recent investigations suggest the possible existence of counter-rotating vortices which are convected by the arc. This phenomenon is currently under investigation and if the internal flow velocities prove to be of the same order as the thermal velocities in the arc, then their contribution to the energy balance should be included.

As noted in Reference 4, the heat flux in typical rail gun plasmas occurs primarily by thermal radiation. In addition, the radiation mean free path λ is $\sim 10^{-4}$m, which is much less than the arc dimensions so that the plasma is relatively opaque to the radiation. Thus, the heat flux can be represented by the "radiative heat conduction equation" [6]

$$\vec{q} = - \frac{4\sigma_s \lambda}{3} \vec{\nabla} T^4 \tag{26}$$

where $\sigma_s = 5.67 \times 10^{-8}$ J/m^{2}deg^{4}s is Stefan's constant. If we assume that the radiation mean free path is a constant, equal to $\bar{\lambda}$, and substitute Equation (26) into Equation (25), we obtain

$$\nabla^2 T^4 = \frac{-3J^2}{4\sigma_s \bar{\lambda} \bar{\sigma}} . \tag{27}$$

Since J is a constant in our model, Equation (27) for T^4 is just Poisson's equation with a constant source term.

If we take the temperature on the arc surface to be a constant T_s then the solution to Equation (27) in the rectangular parallelepiped which represents the arc is given by [7]

$$T^4 = T_s^4 + \sum_{\ell,m,n=0}^{\infty} a_{\ell mn} \sin[(2\ell+1)\pi\xi] \sin[(2m+1)\pi\eta] \sin[(2n+1)\pi\kappa] \tag{28}$$

where ξ, η, and κ represent the nondimensional arc coordinates

$$\xi = x/\ell_a$$

$$\eta = y/W$$

$$\kappa = z/D$$

---

6. Y. B. Zel'dovich and Y. P. Raizer, Physics of Shock Waves and High-Temperature Hydrodynamic Phenomena (Academic, New York, 1966), Vol. I, Chap. 2.
7. H. S. Carslaw and J. C. Jaeger, Conduction of Heat in Solids, Second Edition (Oxford University Press, Oxford, 1980), Chap. 14.

$$a_{\ell mn} = \frac{48J^2}{\sigma_s \bar{\lambda} \bar{\sigma} \pi^5 (2\ell+1)(2m+1)(2n+1)\alpha_{\ell mn}} \tag{29}$$

and

$$\alpha_{\ell mn} = \left(\frac{2\ell+1}{\ell_a}\right)^2 + \left(\frac{2m+1}{W}\right)^2 + \left(\frac{2n+1}{D}\right)^2 . \tag{30}$$

The series in Equation (28) can be evaluated for T at several points within the arc and the resulting values integrated numerically to obtain the average temperature $\bar{T}$. We note, however, that the temperature profile throughout most of the arc is fairly well characterized by the first term in the series. The additional terms serve primarily to define the temperature near the arc boundaries. Thus, we approximate the average arc temperature by

$$\bar{T} = \int_0^1 \int_0^1 \int_0^1 \{T_s^4 + a_{ooo} \sin(\pi\xi)\sin(\pi\eta)\sin(\pi\kappa)\}^{\frac{1}{4}} d\xi d\eta d\kappa \tag{31}$$

where

$$a_{ooo} = \frac{48J^2}{\sigma_s \bar{\lambda} \bar{\sigma} \pi^5 \left(\frac{1}{\ell_a^2} + \frac{1}{W^2} + \frac{1}{D^2}\right)} . \tag{32}$$

If the surface temperature is sufficiently low, the temperature within the interior of the arc is relatively insensitive to T_s. We assume this to be the case and neglect the contribution of T_s to the integral in Equation (31) so that

$$\bar{T} = a_{ooo}^{\frac{1}{4}} \left[\int_0^1 \sin^{\frac{1}{4}}(\pi\xi) d\xi\right]^3 . \tag{33}$$

The integral in Equation (33) is given by [8]

$$\int_0^1 \sin^{\frac{1}{4}}(\pi\xi) d\xi = \frac{1}{\pi} B(5/8, 1/2) = 2.69 \tag{34}$$

---

8. P. J. Davis, "Gamma Function and Related Functions," in Handbook of Mathematical Functions, edited by M. Abramowitz and I. A. Stegun (Dover, New York, 1972).

where B(x,y) is the beta function.

Substituting Equations (32) and (34) into Equation (33) and using the definition of J given by Equation (7) yields the relatively simple expression

$$\bar{T} = .394 \left\{ \frac{j^2}{\sigma_s \bar{\lambda} \bar{\sigma} \left[1 + \left(\frac{\ell_a}{W} \right)^2 + \left(\frac{\ell_a}{D} \right)^2 \right]} \right\}^{1/4} \tag{35}$$

for the average arc temperature.

If we retain only the first term in the series of Equation (28), we can also estimate the maximum arc temperature, which occurs in the center of the arc. The resulting expression is

$$T_{max} = (T_s^4 + a_{ooo})^{1/4}. \tag{36}$$

Again, if T_s is sufficiently low, the maximum arc temperature can be represented by

$$T_{max} = a_{ooo}^{1/4} = 1.59\,\bar{T}. \tag{37}$$

Thus, this simple model suggests that the maximum temperature is roughly 60% higher than the average temperature in the arc.

The values of $\bar{\lambda}$ and $\bar{\sigma}$ used in Equation (35) to evaluate $\bar{T}$ are calculated based on the average arc properties. For a fully ionized plasma, the radiation mean free path can be approximated, in MKS units, by [9]

$$\bar{\lambda} = \frac{4.4 \times 10^{32}\ \bar{T}^{3.5}}{\bar{N}^2\ \bar{\alpha}(1 + \bar{\alpha})^2} \tag{38}$$

where $\bar{N}$ is the average number density of heavy particles and $\bar{\alpha}$ is the average ionic charge in the plasma. We calculate $\bar{N}$ based on the average temperature and pressure in the plasma,

$$\bar{N} = \frac{\bar{p}}{(1 + \bar{\alpha}) k_b \bar{T}}, \tag{39}$$

9. See Reference 6, Chapter 5.

so that $\bar{\lambda}$ can be expressed as

$$\bar{\lambda} = \frac{8.38 \times 10^{-13}\ \bar{T}^{11/2}}{\bar{p}^2\ \bar{\alpha}} \quad . \tag{40}$$

The average degree of ionization is given by

$$\bar{\alpha} = \sum_j j x_j \tag{41}$$

where x_j represents the ratio of the number of atoms ionized j times to the total number of heavy particles. The x_j are obtained from solutions to the Saha equations [10] which can be represented in the form

$$\frac{\bar{\alpha} x_{j+1}}{(1+\bar{\alpha}) x_j} = K_{j+1}(\bar{T},\ \bar{p}) \tag{42}$$

and are calculated based on the average arc temperature and pressure.

To simplify the evaluation of the x_j, it is assumed that for a given set of $\bar{T}$ and $\bar{p}$, the plasma consists only of ions with two separate degrees of ionization. For example, the arc particles may be assumed to be either neutral or singly ionized, or singly or doubly ionized, etc. With this approximation, the Saha equations can be solved explicitly for the fraction x_j.

The average conductivity is calculated from the results of Spitzer, et al. [11-13] for a fully ionized plasma:

---

10. See Reference 4, Chapter 3.
11. L. Spitzer, Physics of Fully Ionized Gases (Interscience, New York, 1965), Chapter 5.
12. R. S. Cohen, L. Spitzer, P. McR. Routly, "The Electrical Conductivity of an Ionized Gas," Phys. Rev. 80, 230 (1950).
13. L. Spitzer and R. Harm, "Transport Phenomena in a Completely Ionized Gas," Phys. Rev. 89, 977 (1953).

$$\bar{\sigma} = \frac{2.63 \times 10^{-2}\ \gamma_e}{Z}\ \bar{T}^{3/2} \left\{ \ln\left[\frac{4.57 \times 10^{-5}\ \bar{T}^2}{Z \sqrt{\bar{\alpha}\ \bar{p}/(1+\bar{\alpha})}} \right] \right\}^{-1} \qquad (43)$$

where

$$Z = \sum_j j^2 x_j \ / \ \sum_j j x_j \qquad (44)$$

and γ_e is a weak function of Z equal to .6833 for Z = 2 and .5816 for Z = 1. As indicated by Equation (43), the average conductivity is calculated based on the average temperature, pressure, and degree of ionization in the arc.

Equations (40) and (43) complete the specification of the problem. The calculation of the arc properties proceeds as follows. For a given geometry, arc mass, projectile mass and current per unit height on the rails, the average pressure and acceleration are calculated from Equations (24) and (20), respectively. The arc length and average arc temperature are then calculated in an iterative fashion. First, values are assumed for ℓ_a and $\bar{T}$. The average conductivity $\bar{\sigma}$ is then calculated from Equation (43) and the radiation mean free path from Equation (40) with the assumed value of $\bar{T}$ and the calculated pressure $\bar{p}$. These values are then substituted into Equation (35) and a new estimate for the temperature obtained. A revised estimate for ℓ_a is obtained from Equation (12) which can be written as

$$\ell_a = \frac{C_1 k_b (1 + \bar{\alpha}) \bar{T}}{a\, m_o} \ . \qquad (45)$$

The procedure is continued until the estimated values of $\bar{T}$ and ℓ_a agree with the calculated values to within some tolerance. In carrying out the calculations it was found that the number of iterations required to obtain convergence was reduced significantly if Equation (35) was rewritten so that the temperature dependence in $\bar{\lambda}$ was transformed to the left-hand-side of the equation. For all the cases considered, convergence to within 0.1% was obtained in less than twenty iterations with this revised calculation technique.

III. APPLICATION OF THE MODEL TO THE RM EXPERIMENT

In this section we will use the model developed in Section II to predict the plasma conditions in the RM experiment. Because it is not possible to determine *a priori* which two Saha equations to use in the calculation, we first calculate the plasma properties assuming only singly ionized and doubly ionized species are present. If the fraction of singly ionized species exceeds 0.5, the calculation is repeated assuming that only neutrals and singly ionized species are present. The calculation which gives the more uniform distribution among the two species is then reported. For the cases which are considered in this report, the results reported for $\overline{T} \lesssim 30{,}000°K$ correspond to solutions where the ions were assumed to be only singly ionized, whereas for $\overline{T} \gtrsim 30{,}000°K$ the results correspond to calculations when the plasma was assumed to consist of only singly and doubly ionized species.

Table I shows the baseline properties used in our simulation of the RM experiment and Table II shows the model's predictions for these baseline conditions. The model predicts an average arc temperature of approximately 35,700°K and a maximum temperature, based on Equation (37), of 56,800°K. These temperatures are comparable to the estimate of 44,000 ± 13,000°K obtained in McNab's analysis [14] of the RM experiment. The average temperature calculated here is approximately a factor of 1.6 lower than the average temperature calculated in Reference 4 based on only axial heat loss. This difference was anticipated in the earlier work and results from the additional radiation losses in the three-dimensional temperature calculation. We note that in our calculation an arc mass was assumed which was twice that used in the analysis of References 4 and 14. The effect of arc mass on the properties of the arc will be discussed in detail in the following section. Here we only note that reducing the arc mass by a factor of two in our calculation increases the average and mean arc temperatures by approximately 14%. Thus, the qualitative agreement with McNab's analysis and the considerably lower prediction compared to the one-dimensional analysis remain valid even for the lower arc mass.

---

14. I. R. McNab, "Electromagnetic Acceleration by a High Pressure Plasma," J. Appl. Phys. 51, 2549 (1980).

TABLE 1. BASELINE CONDITIONS FOR THE RM EXPERIMENT

Symbol	Quantity	Value
W	rail separation	1.27×10^{-2} m
D	effective rail height†	1.56×10^{-2} m
m_p	projectile mass	3.0×10^{-3} kg
j	current per unit height of rail	1.92×10^{7} A/m
m_o	mass of ions and neutrals	1.1×10^{-25} kg
m_a	arc mass	2×10^{-4} kg*

*estimated value

†See Reference [5]

TABLE 2. MODEL PREDICTIONS FOR BASELINE RM PARAMETERS

Symbol	Quantity	Value
$\bar{T}$	average arc temperature	35,700°K
T_{max}	maximum arc temperature	56,800°K
$\bar{p}$	average arc pressure	1.47×10^{8} Nt/m^2
p_f	final arc pressure	2.17×10^{8} Nt/m^2
$\bar{\rho}$	average arc density	12.7 kg/m^3
ρ_f	final arc density	18.7 kg/m^3
ℓ_a	arc length	7.9 cm
a	arc-projectile acceleration	1.43×10^{7} m/s^2
$\bar{n}_e$	average electron number density	1.84×10^{26} /m^3
$\bar{\alpha}$	average degree of ionization	1.59

The arc pressures and the acceleration shown in Table 2 are essentially the same as those calculated in the one-dimensional model. They are approximately a factor of two higher than McNab's estimates, however. The lack of agreement with McNab's calculation arises apparently because the use of infinitely high rails in the present calculation overestimates the force on the projectile. If we equate the force on the projectile, obtained by multiplying Equation (23) by the area WD, to 1/2 L' I^2, where I = jD is the total current in the rails, we can derive an effective inductance per unit length for our model of

$$L' = \mu \frac{m_p W}{(m_a + m_p) D} . \qquad (46)$$

Evaluating Equation (46) for the RM parameters yields a value of approximately .96 μH/m for L'. McNab, on the other hand, uses an effective inductance of .42 μH/m in his calculation of the force on the projectile.

An effective inductance can also be deduced from the RM experimental results. If we neglect the drag on the projectile due to the rails, we can relate the distance traveled by the projectile to the acceleration time by the equation

$$\frac{d^2 s}{dt^2} = \frac{1}{2m_p} L' I^2(t) . \qquad (47)$$

The current can be written as

$$I(t) = I_o e^{-t/\tau} \qquad (48)$$

where I_o is the current at t = 0 and τ is the time constant of the storage inductor which drives the current through the rail gun. Rashleigh and Marshall report that the current fell by 20% during the acceleration time of 1.2×10^{-3}s, which suggests a value of 5.38×10^{-3}s for τ.

The solution to Equation (47) with s(0) = 0 and no initial velocity is

$$s(t) = G \left(\frac{2t}{\tau} + e^{-2t/\tau} - 1 \right) \qquad (49)$$

where

$$G = \frac{\tau^2}{8m_p} L' I_o^2 \ . \qquad (50)$$

Evaluating Equation (49) at the muzzle conditions (s = 5m, $t = 1.2 \times 10^{-3}$s) with I_o = 300 kA and $\tau = 5.38 \times 10^{-3}$s yields a value of 0.53 μH/m for L'. This value is approximately one-half of the value calculated from our model. Part of the difference arises because our assumption of infinitely high rails overestimates the electromagnetic fields in the arc, and thus the force on the projectile. In addition the model neglects any frictional effects on the projectile, which are included implicitly when we derive an inductance from the RM experimental results.

The model predicts an arc length of 7.9 cm, which is approximately 85% of the value obtained in the previous one-dimensional analysis [4]. The reduction in arc length results from the difference in arc temperatures in the two models. To illustrate we note from Equation (12) that the arc length is proportional to

$$\ell_a \propto \frac{m_a(1 + \bar{\alpha})\bar{T}}{am_p} \qquad (51)$$

where we have used the relationship

$$C_1 \propto m_a/m_p \qquad (52)$$

for small values of m_a/m_p. Since the force on the projectile is essentially the same in the two calculations, the ratio of the arc lengths reduces to

$$\frac{\ell_a}{(\ell_a)_{1D}} = \frac{m_a(1 + \bar{\alpha})\bar{T}}{[m_a(1 + \bar{\alpha})\bar{T}]_{1D}} \ . \qquad (53)$$

Although the arc mass used in this calculation is twice that used in the calculation of Reference 4, the average temperature and degree of ionization decreased enough to reduce the ratio in Equation (53) to 0.85.

In general, the model developed here appears to give results which are consistent with the one-dimensional model, except for the expected reduction in the predicted value for the arc temperature. This reduction in temperature also accounts for the only other discrepancy between the two models, the shortening of the arc length. Both models, however, overpredict the acceleration of the projectile due to the assumption of infinitely high rails in calculating the force and the neglect of drag on the projectile.

IV. EFFECT OF PARAMETER VARIATIONS ON ARC PROPERTIES

The model developed in the preceding section is well suited for parametric studies of rail gun plasmas because it is computationally efficient and, in addition, simple enough to be physically transparent. In this section, we will use the model to investigate the range of plasma properties which can be obtained by varying the arc mass, the projectile mass and the rail gun current. To conduct this investigation, we will systematically vary one parameter while keeping the other rail gun parameters fixed at their baseline values for the RM experiment, given by Table 1.

We begin by considering the effect of arc mass on the plasma properties. Figure 3 shows how the maximum and average arc temperatures vary as the arc's mass is increased from 0.06 g to 3.0 g, the upper limit being the projectile mass for the RM experiment. A decrease in the arc mass results in an increase in the arc temperature, as can be seen from the figure, primarily because there are fewer particles to absorb the ohmic heating of the arc. The increase in temperature is not large, however, because the radiation losses, which vary as T^4, inhibit large increases in the arc temperature. For example, although the arc mass varies by almost two orders of magnitude in Figure 3, the average arc temperature changes only by roughly a factor of 2 varying between 20,000°K and 44,000°K. Over the same range of m_a, the maximum arc temperature varies from 32,000°K to 70,000°K.

Figure 4 shows the effect of the arc mass on the average pressure $\bar{p}$, the maximum pressure p_{max}, and the final pressure at the projectile p_f. According to the figure, a decrease in arc pressure accompanies an increase in arc mass. However, for $m_a/m_p \ll 1$ the pressure in the arc is relatively insensitive to variations in arc mass with $\bar{p} \sim 1.5 \times 10^8 Nt/m^2$ and $p_{max} \sim p_f \sim 2.3 \times 10^8 Nt/m^2$. As the arc mass becomes comparable to the projectile mass ($m_a \gtrsim 0.5$ g), the pressure becomes more sensitive to the arc mass. In addition, the difference between the final pressure and the maximum pressure becomes noticeable. For an arc mass equal to the projectile mass the average pressure is 70% of its asymptotic value at small m_a, whereas the pressure at the projectile is only approximately 50% of its asymptotic value.

Figure 5 shows the effect of arc mass on the length of the arc and on the common acceleration of the arc and

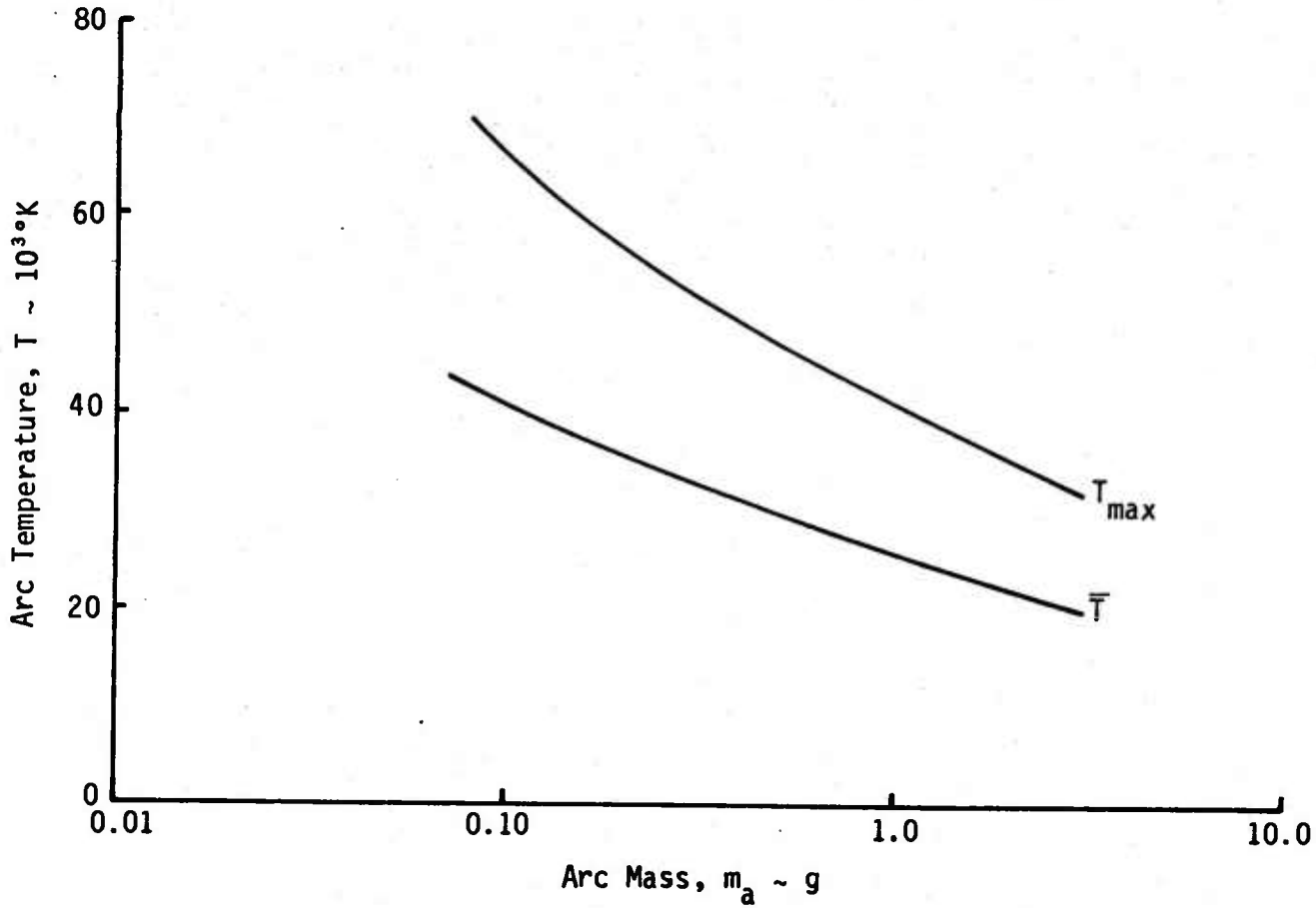

Figure 3. Effect of Arc Mass on Maximum and Average Arc Temperatures (RM Parameters)

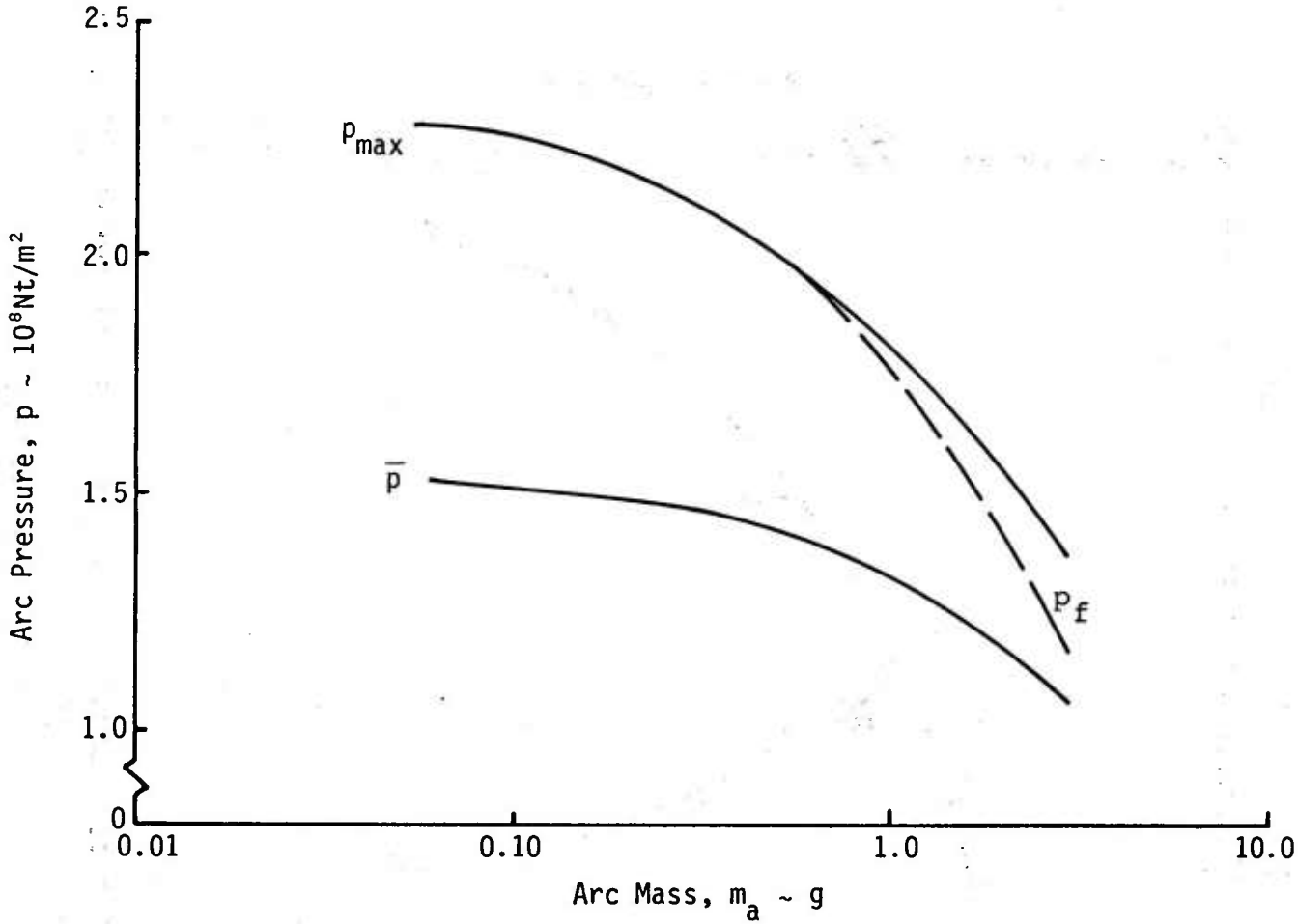

Figure 4. Effect of Arc Mass on Arc Pressures (RM Parameters)

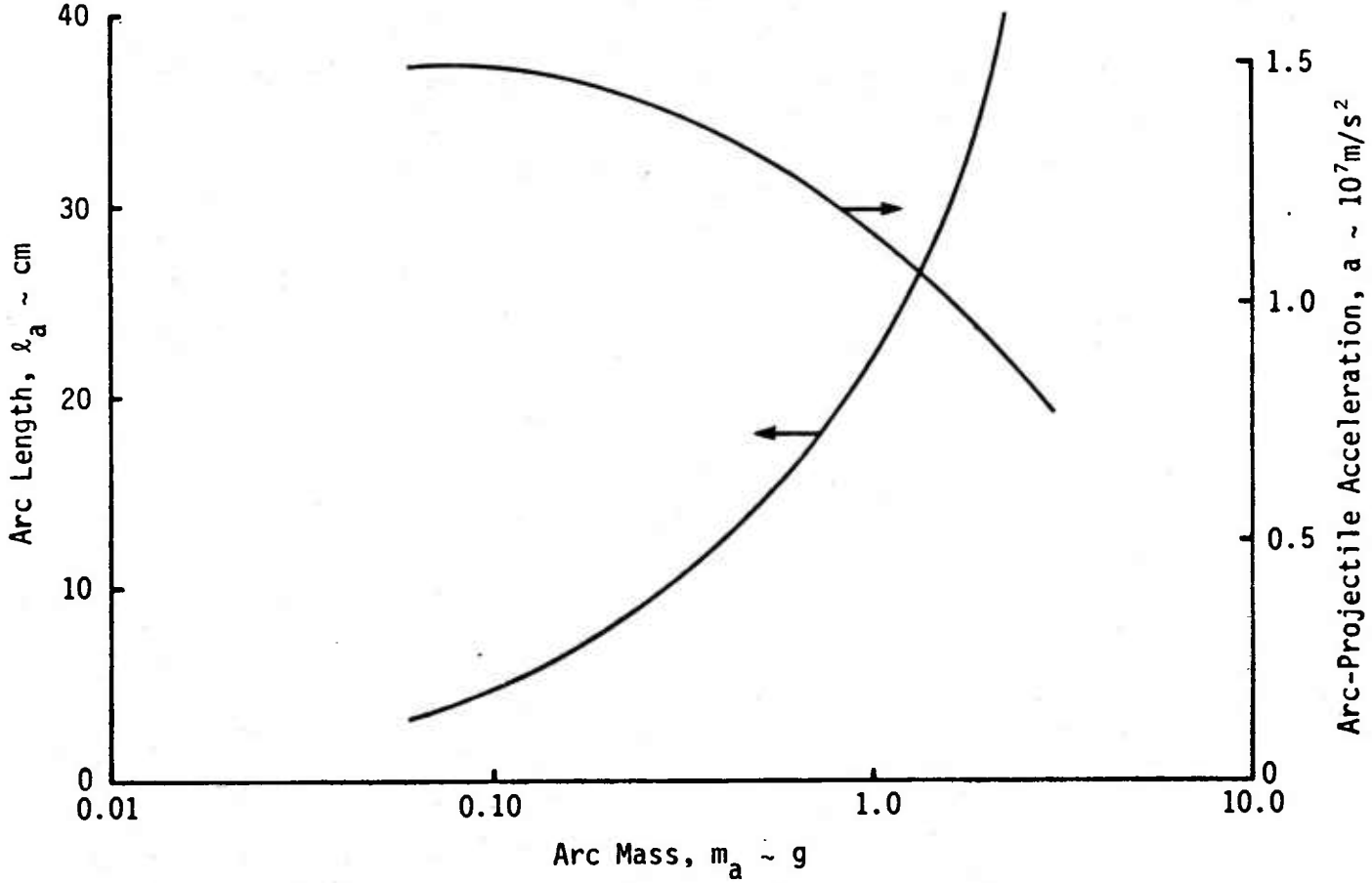

Figure 5. Effect of Arc Mass on Arc Length and Acceleration (RM Parameters)

projectile. According to the figure, the arc length is very sensitive to arc mass increasing from 3.1 cm at m_a = .06 g to 51.0 cm at m_a = 3 g. The acceleration which is proportional to p_f is considerably less sensitive to the value of m_a. Over the same range of m_a it falls from 1.5×10^7 m/s^2 to 0.8×10^7 m/s^2.

In summary we find that an increase in arc mass is accompanied by decreases in the arc temperature, pressure, and acceleration, and by an increase in the arc length. The arc length is, by far, the arc property most sensitive to m_a. For values of $m_a/m_p << 1$, the arc pressures and consequently the acceleration are relatively insensitive to the arc mass. In fact for $m_a/m_p << 1$ variations in the arc mass affect ℓ_a the most, the temperature to a lesser extent, and the acceleration even less. These results are particularly encouraging since present methods of generating the arc by exploding a copper fuse provide little control over the mass eventually contained within the arc.

There is somewhat greater freedom in choosing the projectile mass and we will now investigate its effect on the properties of the arc. In Figures 6 and 7 we show the effect of m_p on the arc temperatures and pressures, respectively. Figure 8 shows the effect of m_p on the arc length and the acceleration. Recalling that m_a = 0.2 g for these calculations we note that the arc's thermodynamic properties as well as its length are independent of the projectile mass for $m_a/m_p << 1$. Because p_f remains constant, the acceleration of the arc and projectile must fall as $1/m_p$ in this region and this behavior is evident in Figure 8. For a projectile mass on the order of the arc mass we see a decrease in arc pressure and temperature and an increase in arc length with decreasing m_p.

Finally, we investigate the effect of varying the rail gun current on the arc properties. Figure 9 shows how the average arc temperature and the maximum arc temperature vary with j, the current per unit height of rail. We note from the figure that the average arc temperature increases approximately linearly from 20,000°K to 50,000°K as j increases from 1.0×10^7 A/m to 3.0×10^7 A/m. Similarly, the maximum temperature increases from 32,000°K to 80,000°K. The increase in temperature with increasing j occurs, of course, because of the increased ohmic heating of the arc.

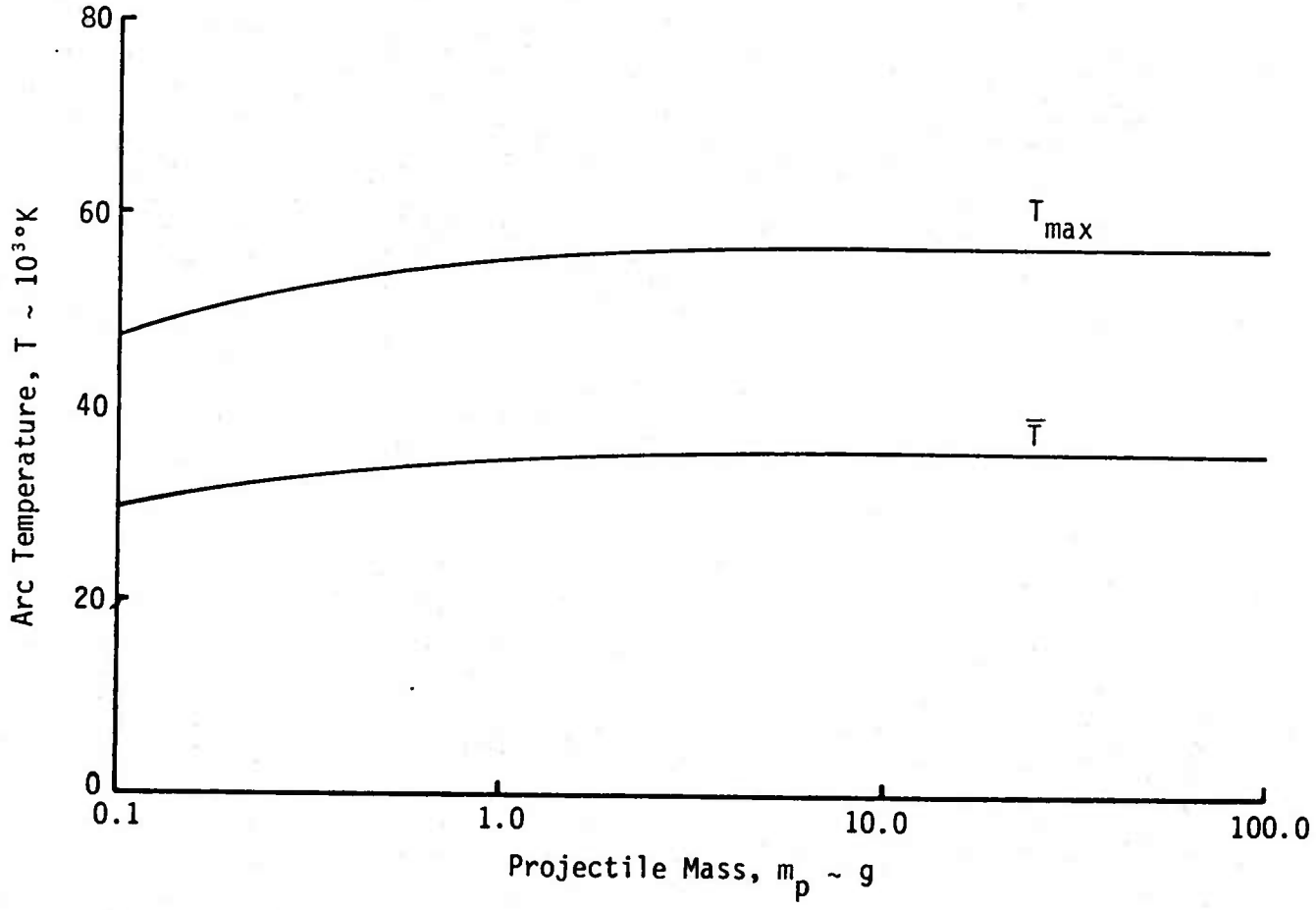

Figure 6. Effect of Projectile Mass on Maximum and Average Arc Temperatures (RM Parameters)

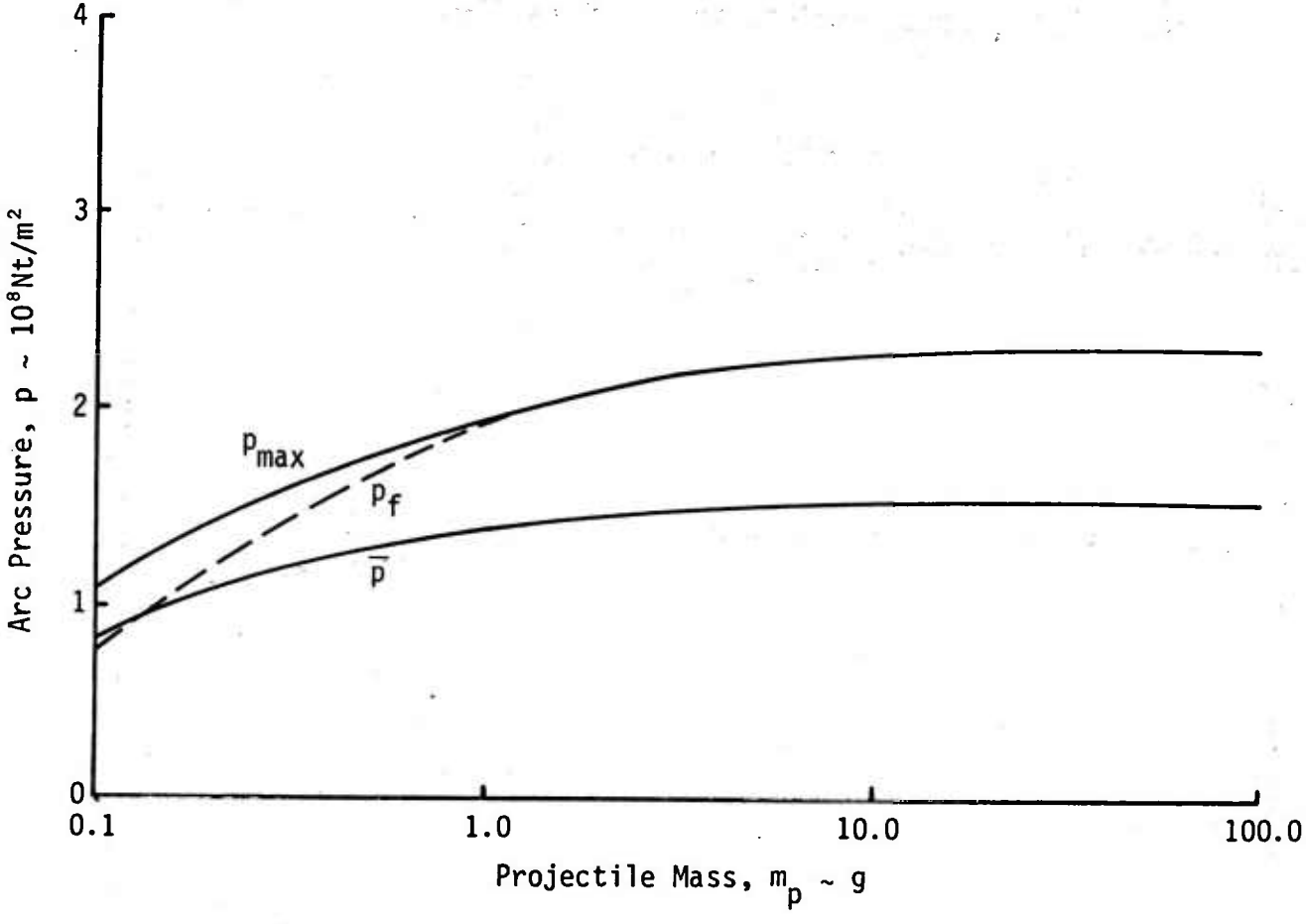

Figure 7. Effect of Projectile Mass on Arc Pressures (RM Parameters)

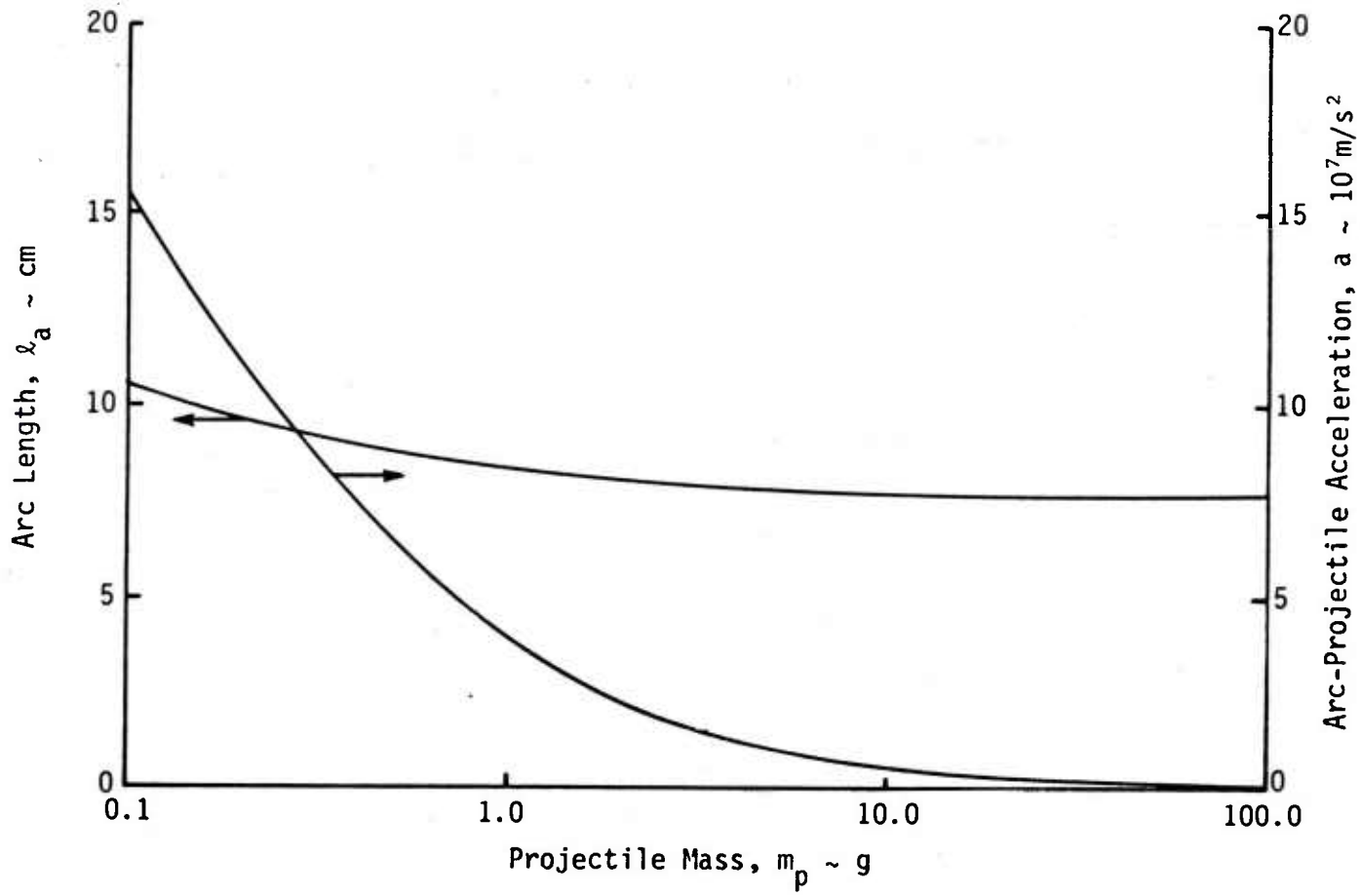

Figure 8. Effect of Projectile Mass on Arc Length and Acceleration (RM Parameters)

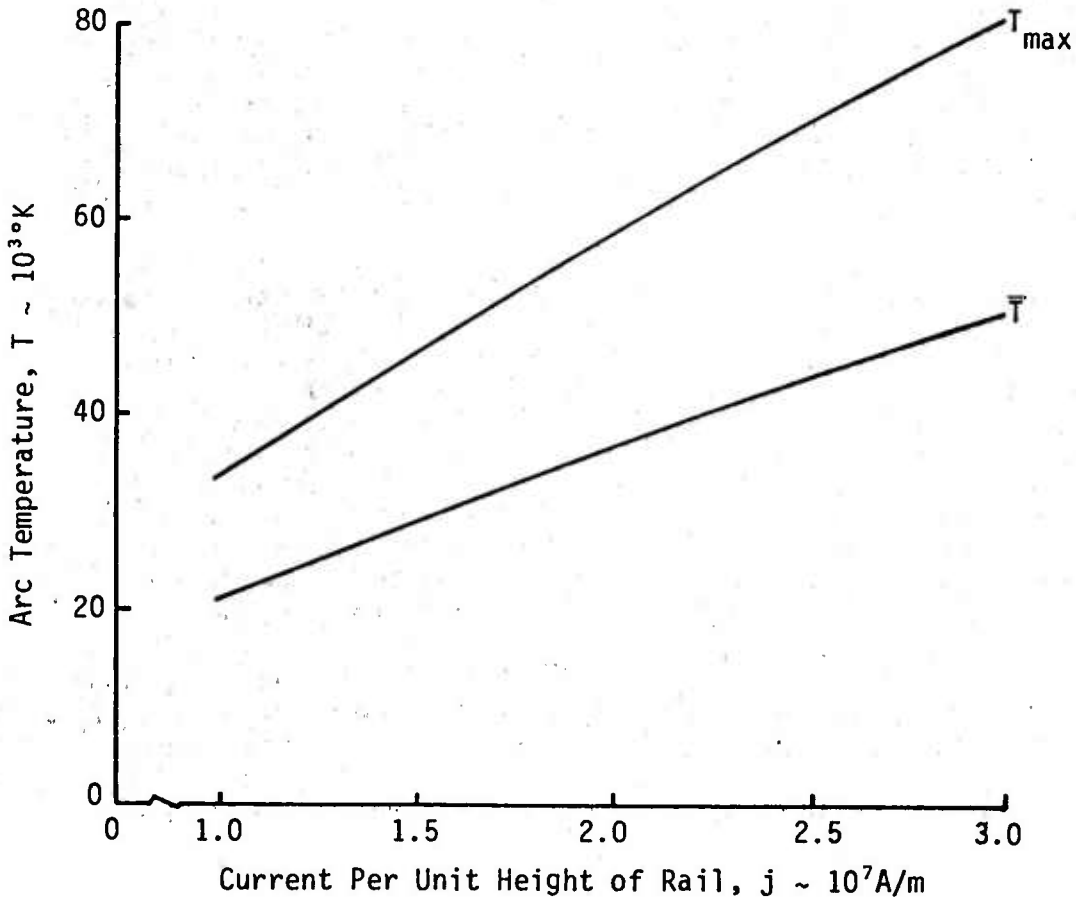

Figure 9. Effect of Current on Maximum and Average Arc Temperatures (RM Parameters)

Figure 10 shows the effect of current on the arc pressures, p_{max} and $\bar{p}$. For the RM parameters, $m_a/m_p << 1$ and the model predicts that $\bar{p} = 1/3\ \mu j^2$ and $p_f = p_{max} = 1/2\ \mu j^2$. Figure 10 merely expresses these relationships graphically.

In Figure 11 we show the effect of varying the current on the arc length and the acceleration. The acceleration also increases as j^2 since it is linearly related to p_f for a constant projectile mass. The arc length is considerably less sensitive to j; it varies only between 5.0 cm and 11.0 cm for the range of currents shown in the figure. This behavior can be understood by referring to Equation (51) which shows that ℓ_a is proportional to the arc temperature and inversely proportional to the acceleration and both parameters increase with increasing j.

According to the results presented in Figures 3 - 11 the model predicts that rail gun arcs will typically have arc lengths on the order of one to tens of centimeters, average temperatures in the range of 20,000°K to 40,000°K, and pressures on the order of $10^8 Nt/m^2$. The arc acceleration is, of course, strongly dependent on the combined arc and projectile masses but typically a ~ 10^7 m/s^2 and 10^8 m/s^2 for combined masses on the order of 1 g and 0.1 g, respectively. In addition, for $m_a/m_p << 1$ which is typically the case in conventional rail gun experiments, the arc pressure is a function primarily of the current.

The arc length and arc temperatures depend primarily on the arc mass and the current. $\bar{T}$ decreases with increasing m_a and increases with increasing m_p, while ℓ_a has the opposite behavior. And, finally, for $m_a/m_p << 1$, the acceleration is determined primarily by the current and, of course, the projectile mass m_p.

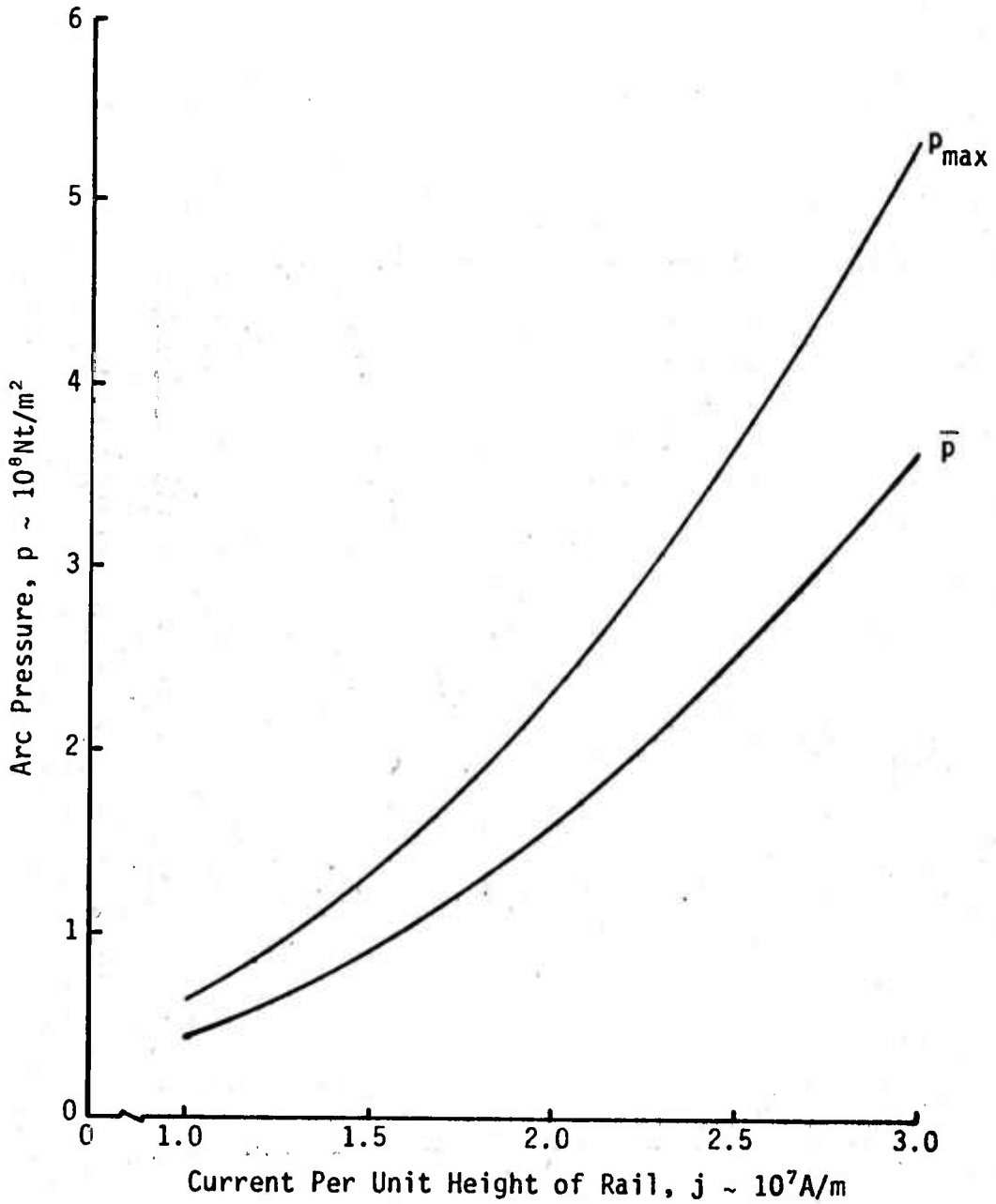

Figure 10. Effect of Current on Arc Pressures (RM Parameters)

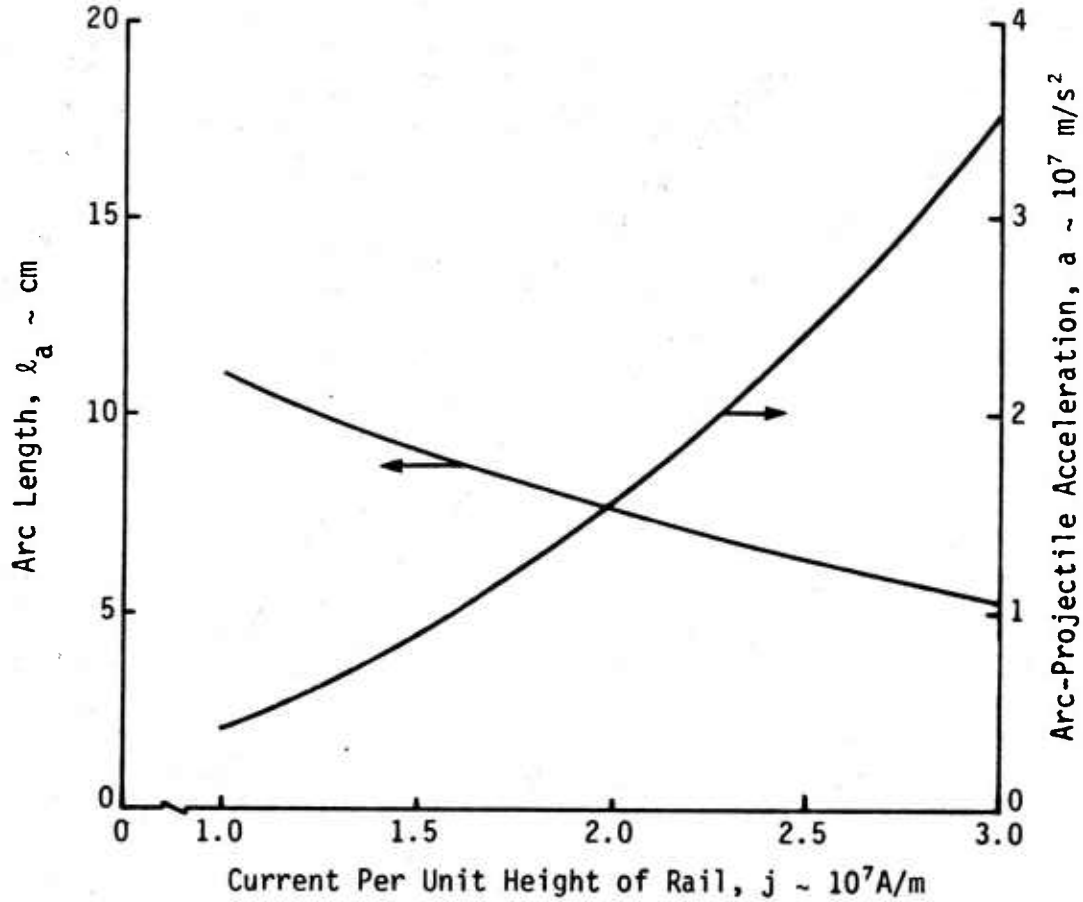

Figure 11. Effect of Current on Arc Length and Acceleration (RM Parameters)

V. APPLICATION OF MODEL TO THE PROPOSED WESTINGHOUSE EXPERIMENT

Westinghouse is currently building a rail gun which it proposes to use to accelerate projectiles significantly heavier than the one used in the RM experiment. The model described in this report was used to predict the arc properties for the set of conditions given in Table 3, which are comparable to the conditions for the proposed Westinghouse experiment.

TABLE 3. PARAMETERS FOR THE PROPOSED WESTINGHOUSE EXPERIMENT

Symbol	Quantity	Value
W	rail separation	5×10^{-2} m
D	rail height	5×10^{-2} m
m_p	projectile mass	0.3 kg
j	current per unit height of rail	1.47×10^{7} A/m

Figures 12 and 13 show the results of the analysis for the arc temperature and the arc length. Since little control can be exercised over the arc mass, we have plotted these parameters as a function of m_a, with values ranging from 0.5 g to 30.0 g. We note that over this range, the average arc temperature varies from 23,000°K to 45,000°K and the arc length from 4 to over 50 cm. These plasma properties are not much different from those shown in Figures 3 and 5 for the RM experiment although we note that in the RM experiment they correspond to arc masses from 0.05 g to 3.0 g. If we compare the arc properties at the same arc mass, say m_a = 0.5 g, we find that the temperatures for the proposed Westinghouse parameters are approximately 1.5 times the temperatures for the RM parameters while the arc length is a fourth as large.

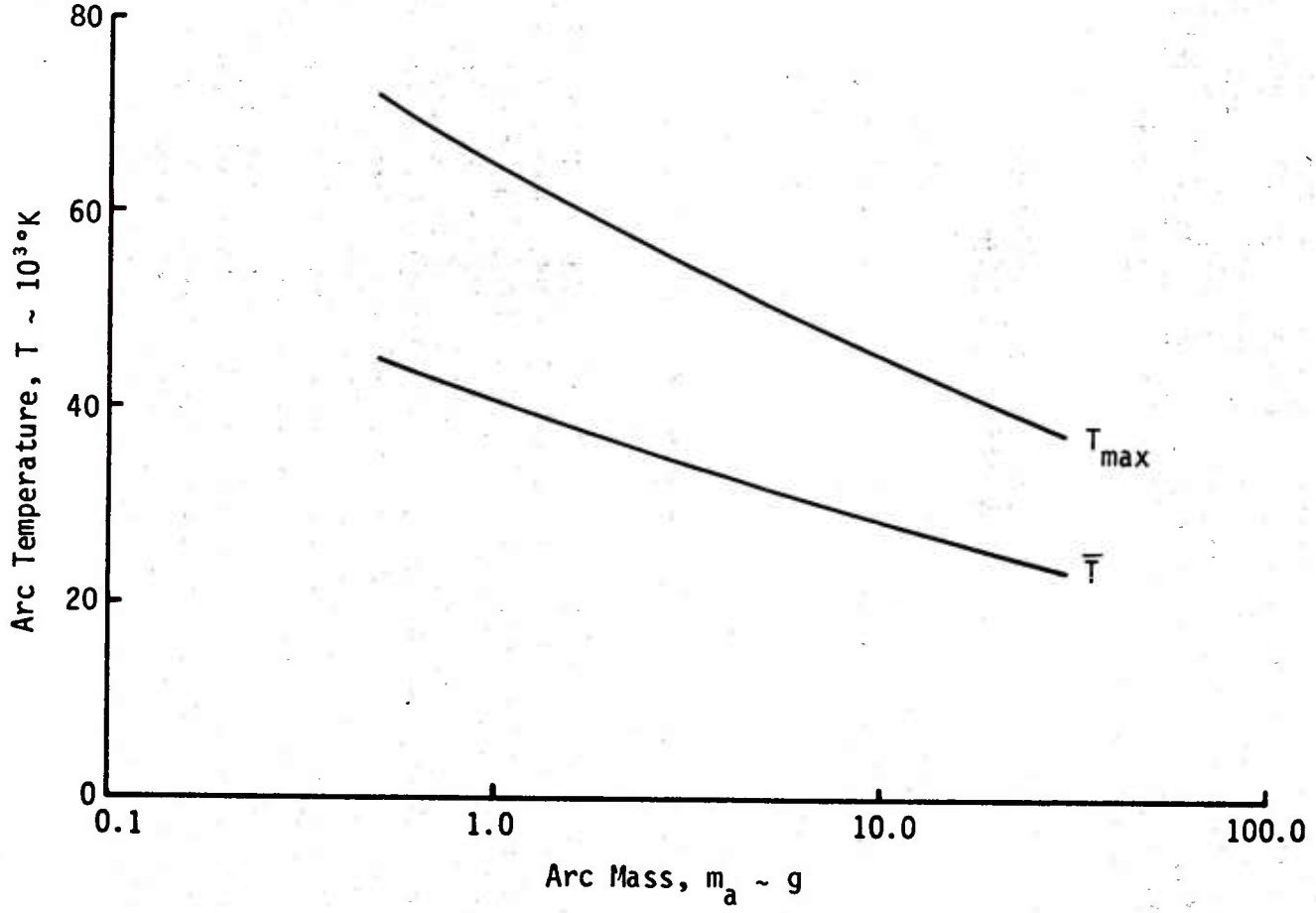

Figure 12. Effect of Arc Mass on Arc Temperature for the Westinghouse Experiment

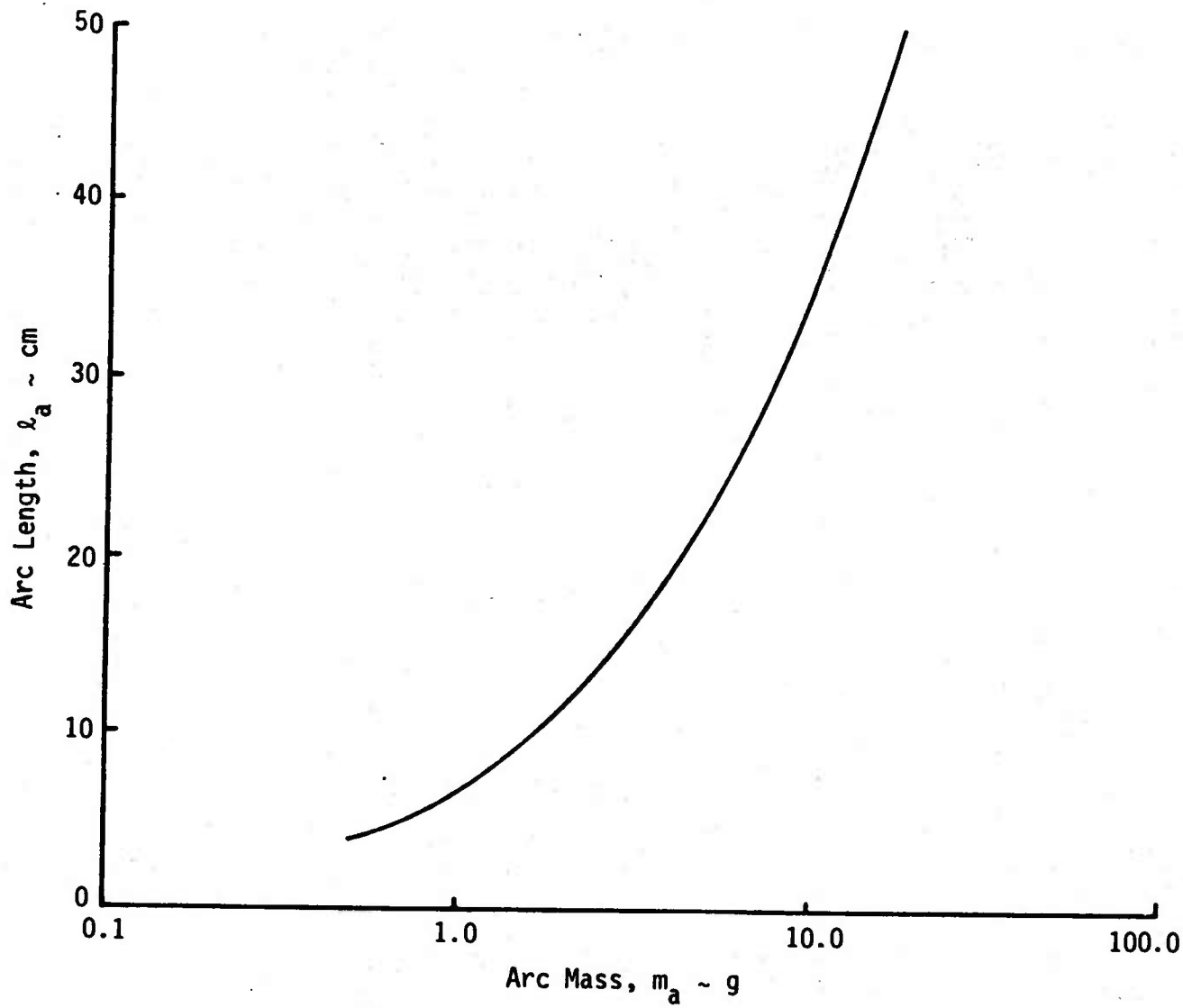

Figure 13. Effect of Arc Mass on Arc Length for the Westinghouse Experiment

VI. EFFECTIVE RANGE OF RAIL GUN PLASMAS

In the preceding sections we have investigated the range of plasma properties which can be attained with current rail gun technology. It is possible, at least conceptually, to use the rail gun as a plasma accelerator by removing the projectile from the path of the arc at the muzzle. Alternatively, the projectile could be designed to melt during the acceleration process and become part of the plasma.

The utility of a plasma accelerator will be determined to a certain extent by how quickly the plasma dissipates once it leaves the muzzle. Although the plasma pressures are typically on the order of 10^3 atmospheres the plasma remains confined to a relatively small volume while in the gun because of the electromagnetic force and the mechanical forces imposed by the rails and projectile. Once it exits the gun, however, these influences are no longer present and the plasma will expand and cool until it achieves mechanical and thermal equilibrium with the surrounding air.

An accurate description of this relaxation process requires the solution of the unsteady fluid dynamics equations with proper account taken of the radiation cooling and the plasma recombination. Such an analysis is beyond the scope of this effort. Rather, here we will take the useful lifetime of the plasma to be the time required for an acoustic wave to traverse the original width W of the plasma which is indicative of the time required for the plasma to expand and establish pressure equilibrium with the surrounding air. (We are assuming here that the height of the rails is approximately equal to the distance between the rails, i.e., W = D, and that both are less than the arc length ℓ_a.)

The acoustic transit time based on the average arc temperature is

$$t_a = W \left[\frac{m_o}{\gamma (1 + \bar{\alpha}) k_b \bar{T}} \right]^{\frac{1}{2}} \qquad (54)$$

where γ is the ratio of specific heats. For this analysis we will assume a value of 5/3 for γ, which corresponds to the specific heat ratio for a perfect monotomic gas.

We define the effective range of the plasma to be the distance traveled by the arc within an acoustic transit time, t_a, after exiting the muzzle. We calculate this distance based on the assumption that the plasma velocity remains constant during the expansion process with a value equal to its velocity at the muzzle. For a constant acceleration, a, the exit velocity is

$$v_e = (2aL)^{\frac{1}{2}} \tag{55}$$

where L is the length of the rail-gun accelerator. The effective range, R, is then the product of v_e and t_a or

$$R = W^2 \left[\frac{m_o \mu j^2 L}{(m_a + m_p)\gamma(1+\bar{\alpha})k_b \bar{T}} \right]^{\frac{1}{2}}. \tag{56}$$

In writing Equation (56) we have substituted Equation (20) for the acceleration with the assumption that W = D.

As an example we calculate R for the RM parameters in Table 1 except for the projectile mass, m_p, which we take equal to 0.2 g, the arc mass. For this case we obtain an average temperature of 30,200°K as shown in Figure 6 and $\bar{\alpha} = 1.35$. Assuming W = D = 1.56 cm and substituting into Equation (56) yields the following expression for the effective range:

$$R = .068\ L^{\frac{1}{2}} \tag{57}$$

where both R and L are expressed in meters.

For a typical accelerator length of 6m, Equation (57) indicates an effective range of 0.2m. Although this range may be sufficient for laboratory studies of plasma properties or for manufacturing applications, it severely limits the possibility of using the arc as a military weapon.

For the arc to be a viable weapon its range would have to be increased by three to four orders of magnitude above that calculated for the RM experiment. Examination of Equation (56) suggests that it would be difficult to achieve such a large increase in range for realistic variations of the rail gun parameters. Thus, extended ranges for rail gun plasmas will have to rely on forces, applied external to the gun, which will counter the radial expansion due to the high internal pressure in

the arc. If confinement of rail-gun arcs can be achieved it will probably result from the interaction of electromagnetic fields with the arc. Electromagnetic fields are frequently used in the laboratory, for example in fusion experiments, to confine plasmas and it may be possible to extend these techniques to a plasma propagating in the atmosphere.

A well-defined plasma propagating through the atmosphere would appear similar, at least superficially, to ball lightning. This observation prompted a review of ball lightning phenomena to determine if the mechanisms responsible for the propagation of ball lightning might be relevant for rail gun arcs. Unfortunately, due to the rare and unpredictable occurrence of ball lightning, there is little experimental data available. The "data" which does exist consists of descriptions, or photographs at best, of individual sightings [15], and several of these have been discredited as representing ball lightning phenomena.

Several techniques including the use of radio frequency discharges have been used to generate plasmas in the laboratory which are similar in appearance to ball lightning. These experiments as well as the actual sightings suggest that ball lightning may be a region of air at atmospheric pressure or slightly less heated to temperatures of a few thousand degrees Kelvin. These thermodynamic properties are quite different from the high temperatures and pressures one would expect in rail gun arcs.

A variety of mechanisms have been proposed to account for the propagation of ball lightning. Some studies suggest the motion of ball lightning may be due to the buoyancy forces exerted on a lighter-than-air plasma. Others speculate that the bright moving glow is caused not by any mass motion but by an ionization front which moves in response to an electromagnetic field.

The current uncertainty regarding the nature of ball lightning and the probable differences between the thermodynamic properties of ball lightning and rail gun arcs suggest that studies of ball lightning phenomena will have little relevance to propagating and confining rail gun plasmas.

---

15. See, for example, J. D. Barry, Ball Lightning and Bead Lightning (Plenum, New York, 1980) for a review of ball lightning phenomena.

VII. CONCLUSIONS AND RECOMMENDATIONS

In this report we have developed a simple, computationally efficient model which can be used to calculate the arc properties for a conventional rail gun ($m_a << m_p$) or for a plasma accelerator ($m_a \simeq m_p$). The model was applied to variations about the RM experimental parameters to determine the effect of arc mass, projectile mass and current density on the arc properties. The model predicts that rail gun arcs typically will have arc lengths on the order of one to tens of centimeters, average temperatures from 20,000°K to 40,000°K and pressures on the order of 10^8 Nt/m^2. In addition, for the conventional rail gun ($m_a << m_p$) the pressure is a function primarily of the current whereas the arc length and arc temperature depend on both the arc mass and the current. In general, the arc temperature decreases with increasing arc mass and increases with increasing projectile mass, while the arc length exhibits the opposite behavior.

Comparison of the model predictions with the results of the RM experiment indicates that the arc-projectile acceleration is overestimated by a factor of about 2. One reason for this discrepancy is the use of infinitely high rails in the model, an assumption which results in an overestimate of the force on the projectile. In addition, the drag on the projectile due to the rails was neglected in the calculation. In future work it would be desirable to modify the present model to account for the effect of finite rail height on the acceleration and to investigate the effect of frictional forces on the projectile.

The effective range of rail gun plasmas was estimated based on the acoustic transit time across the arc. The calculation suggests an effective range on the order of a few tens of centimeters for typical rail gun parameters. While this range may be sufficient for laboratory experiments or manufacturing applications it precludes the use of the plasma as a weapon unless some technique for limiting the plasma expansion can be found. An investigation of the literature on ball lightning revealed little information relevant to maintaining confined rail gun plasmas in the atmosphere. Future studies of the plasma accelerator as a weapon should focus on techniques, such an electromagnetic confinement, for limiting the expansion of the arc as it propagates in the atmosphere.

This task was performed for the U.S. Army Armament Research and Development Command. Dr. John D. Powell of the Ballistic Research Laboratory served as the Contracting Officer's Technical Representative. The author acknowledges, with appreciation, the technical discussions with Dr. Powell on rail gun technology as well as prepublication access to his work.

REFERENCES

1. S. C. Rashleigh and R. A. Marshall, "Electromagnetic Acceleration of Macroparticles to High Velocities," J. Appl. Phys. 49, 2540 (1978).

2. R. A. Marshall, "The Australian National University Rail Gun Project," Atomic Energy, 16, January 1975.

3. J. P. Barber, "The Acceleration of Macroparticles and a Hypervelocity Electromagnetic Accelerator," Ph.D. Thesis (Australian National University, 1972) (Unpublished).

4. J. D. Powell and J. H. Batteh, "Plasma Dynamics of an Arc-Driven, Electromagnetic Projectile Accelerator," J. Appl. Phys. 52, 2717 (1981).

5. J. D. Powell and J. H. Batteh, "Plasma Dynamics of the Arc-Driven Rail Gun," Ballistic Research Laboratory Report No. ARBRL-TR-02267, 1980. (AD A092345)

6. Y. B. Zel'dovich and Y. P. Raizer, Physics of Shock Waves and High-Temperature Hydrodynamic Phenomena (Academic, New York, 1966), Vol. I, Chapter 2.

7. H. S. Carslaw and J. C. Jaeger, Conduction of Heat in Solids, Second Edition (Oxford University Press, Oxford, 1980), Chapter 14.

8. P. J. Davis, "Gamma Function and Related Functions," in Handbook of Mathematical Functions, edited by M. Abramowitz and I. A. Stegun (Dover, New York, 1972).

9. See Reference 6, Chapter 5.

10. See Reference 4, Chapter 3.

11. L. Spitzer, Physics of Fully Ionized Gases (Interscience, New York, 1965) Chapter 5.

12. R. S. Cohen, L. Spitzer, P. McR. Routly, "The Electrical Conductivity of an Ionized Gas," Phys. Rev. 80, 230 (1950).

13. L. Spitzer and R. Harm, "Transport Phenomena in a Completely Ionized Gas," Phys. Rev. 89, 977 (1953).

14. I. R. McNab, "Electromagnetic Acceleration by a High Pressure Plasma," J. Appl. Phys. 51, 2549 (1980).

15. See, for example, J. D. Barry, Ball Lightning and Bead Lightning (Plenum, New York, 1980) for a review of ball lightning phenomena.

DISTRIBUTION LIST

No. of Copies	Organization
12	Commander Defense Technical Info Center ATTN: DDC-DDA Cameron Station Alexandria, VA 22314
1	Office Under Secretary of Defense Res & Engr ATTN: Mr. Ray Thorkildsen Room 3D1089, Pentagon Washington, DC 20301
1	Deputy Under Secretary of Defense Res & Engr ATTN: Dr. Arden L. Bement Room 3E144, Pentagon Washington, DC 20301
4	Director Defense Advanced Research Projects Agency ATTN: Dr. Joseph Mangano Dr. Gordon P. Sigman Dr. Raymond P. Gogolewski Dr. Harry Fair 1400 Wilson Blvd Arlington, VA 22209
1	Office of Assistant Secretary of the Army ATTN: RDA, Dr. Joseph Yang Room 2E672, Pentagon Washington, DC 20310
1	HQDA (DAMA-ARZ-A, Dr. Marvin Lasser) Washington, DC 20310
1	Commander US Army Materiel Development & Readiness Command ATTN: DRCDMD-ST 5001 Eisenhower Avenue Alexandria, VA 22333
1	Commander US Army Materiel Development & Readiness Command ATTN: DRCLDC, Mr. T. Shirata 5001 Eisenhower Avenue Alexandria, VA 22333
5	Commander US Army Armament Research and Development Command ATTN: DRDAR-TSS (2 cys) DRDAR-LCA, Mr. J.A. Bennett DRDAR-LCA, Dr. T. Gora DRDAR-LCA, Dr. P. Kemmy Dover, NJ 07801
1	Commander US Army Armament Materiel Readiness Command ATTN: DRSAR-LEP-L, Tech Library Rock Island, IL 61299
1	Director US Army ARRADCOM Benet Weapons Laboratory ATTN: DRDAR-LCB-TL Watervliet, NY 12189
1	Commander US Army Aviation Research & Development Command ATTN: DRDAV-E 4300 Goodfellow Blvd. St. Louis, MO 63120
1	Director US Army Air Mobility Research & Development Laboratory Ames Research Center Moffett Field, CA 94035
1	Commander US Army Communications Research & Development Command ATTN: DRDCO-PPA-SA Fort Monmouth, NJ 07703

DISTRIBUTION LIST

No. of Copies	Organization
2	Commander US Army Electronics R&D Command Technical Support Activity ATTN: DELSD-L Fort Monmouth, NJ 07703
2	Commander US Army Missile Command ATTN: DRSMI-R DRSMI-YDL Redstone Arsenal, AL 35809
1	Commander US Army Tank Automotive Research & Development Command ATTN: DRDTA-UL Warren, MI 48090
1	Director US Army TRADOC Systems Analysis Activity ATTN: ATAA-SL, Tech Library White Sands Missile Range, NM 88002
2	Commander US Army Research Office ATTN: Dr. Fred Schmiedeshoff Dr. M. Ciftan PO BOX 12211 Research Triangle Park, NC 27709
1	Commander Naval Air Systems Command ATTN: Dr. Richard J. Wasneski Code 350F Washington, DC 20360
1	Commander US Naval Research Laboratory ATTN: Code 4770 Washington, DC 20375
2	Commander Naval Surface Weapons Center ATTN: Henry B. Odom, Code F-12 Dr. M. Franklin Rose, Code F-04 Dahlgren, VA 22448
2	AFATL (Dr. Dale M. Davis, Virgil Miller) Eglin AFB, FL 32542
1	AFWL (Dr. William L. Baker) Kirtland AFB, NM 87117
1	AFAPL (Dr. Charles E. Oberly) Wright-Patterson AFB, OH 45433
1	Director Brookhaven National Laboratory ATTN: Dr. James R. Powell Bldg 129 Upton, NY 11973
1	Director Lawrence Livermore National Laboratory ATTN: Dr. Ronald S. Hawke, L-156, Box 808 Livermore, CA 94550
2	Director Los Alamos Scientific Laboratory ATTN: Dr. Clarence M. Fowler, MS970 Dr. Denis R. Peterson, MS985 Los Alamos, NM 87545
1	International Applied Physics ATTN: Dr. John P. Barber 2400 Glenheath Drive Kettering, OH 45440
1	JAYCOR ATTN: Dr. Derek Tidman 205 S. Whiting Street Alexandria, VA 22304

DISTRIBUTION LIST

No. of Copies — Organization

2 R&D Associates
ATTN: Mr. Ronald Cunningham
Dr. Peter Turchi
PO Box 9695
4640 Admiralty Way
Marina Del Rey, CA 90291

1 Science Applications, Inc.
ATTN: Dr. Jad H. Batteh
6600 Powers Ferry RD
Suite 220
Atlanta, GA 30339

1 Science Applications, Inc.
Corporate Headquarters
ATTN: Dr. Frank Chilton
1250 Prospect Plaza
La Jolla, CA 92037

1 Systems Planning Corporation
ATTN: Mr. Andrus Villu
1500 Wilson Boulevard
Arlington, VA 22209

1 Westinghouse Research and Development Laboratory
ATTN: Dr. Ian R. McNab
1310 Beulah RD
Pittsburgh, PA 15253

No. of Copies — Organization

2 Massachusetts Institute of Technology
Francis Bitter National Magnet Laboratory
ATTN: Dr. Henry H. Kolm,
Mr. Peter Mongau
NW-14-3102
170 Albany Street
Cambridge, MA 02139

2 University of Florida
Department of Engineering Sciences
ATTN: Professor K.T. Millsaps
Professor B.M. Leadon
Gainesville, FL 32603

1 University of Tennessee Space Institute
ATTN: Professor D.R. Keefer
Tullahoma, TN 37388

2 University of Texas
Center for Electromechanics
ATTN: Dr. Richard A. Marshall
Mr. William F. Weldon
167 Taylor Hall
Austin, TX 78712

Aberdeen Proving Ground

Dir, USAMSAA
ATTN: DRXSY-D
DRXSY-MP, H. Cohen
Cdr, USATECOM
ATTN: DRSTE-TO-F
Dir, USACSL, Bldg E3516
ATTN: DRDAR-CLB-PA

USER EVALUATION OF REPORT

Please take a few minutes to answer the questions below; tear out this sheet, fold as indicated, staple or tape closed, and place in the mail. Your comments will provide us with information for improving future reports.

1. BRL Report Number _____

2. Does this report satisfy a need? (Comment on purpose, related project, or other area of interest for which report will be used.)

_____

_____

_____

3. How, specifically, is the report being used? (Information source, design data or procedure, management procedure, source of ideas, etc.) _____

_____

_____

4. Has the information in this report led to any quantitative savings as far as man-hours/contract dollars saved, operating costs avoided, efficiencies achieved, etc.? If so, please elaborate.

_____

_____

5. General Comments (Indicate what you think should be changed to make this report and future reports of this type more responsive to your needs, more usable, improve readability, etc.) _____

_____

_____

_____

6. If you would like to be contacted by the personnel who prepared this report to raise specific questions or discuss the topic, please fill in the following information.

Name: _____

Telephone Number: _____

Organization Address: _____

_____

_____